Journal of the Korean Nuclear Society
Volume 30, Number 6, pp.507~517, December 1998

A Calculation Model for Fuel Constituent Redistribution and Temperature Distribution on Metallic U-10Zr Fuel Slug of Liquid Metal Reactors

Cheol Nam and Woan Hwang
Korea Atomic Energy Research Institute
150 Duckjin-dong, Yusong-gu, Taejon 305-353, Korea

(Received October 10, 1997)

Abstract

Unlike conventional fuel types, fuel constituent redistribution and sodium intrusion into the fuel slug are the unique phenomena of the irradiated metallic fuel. A thermal calculation model on metallic U-10 wt.%Zr fuel rod for LMRs is developed with considerations given to these phenomena. The amount of constituent redistribution is estimated based on the thermotransport process. The temperature profile of fuel slug is predicted by taking into account of Zr redistribution, porosity formation and sodium logging effects. A sample calculation is performed and compared to experimental data in literature. As a result, the predicted redistribution and temperature profile are well agreed with experimental data, assuming that 15 times increment of ex-reactor diffusivity, Q_r^* is -50 kJ/mole and sodium is infiltrated only outside of the fuel slug. Furthermore, the redistribution effects on fuel integrity and fuel temperature profile are discussed.

1. Introduction

Recently the potential use of metallic fuel for liquid metal reactors has enhanced owing to the discovery of its merits in safety, high burnup achievement and simple fabrication by extensive investigation of Argonne National Laboratory (ANL) as a part of Integral Fast Reactor (IFR) program[1]. In metallic fuel design, a large sodium-filled gap is provided to permit a good heat removal as well as allowing sufficient volume for expansion. The typical design of metallic fuel pin is shown in Fig. 1. The Korea Atomic Research Institute (KAERI) has been developing the Korea Advanced Liquid Metal Reactor (KALIMER), and its start-up fuel was potentially chosen as sodium bonded U-10 wt.%Zr metallic alloys. As one of the KALIMER activities, the metallic fuel performance code MACSIS[2] has been developed to specify design limits and to assure reliable performance of the fuel pin.

The prediction of the fuel temperature distribution is one of the most important factors in a fuel performance code since fuel temperature affects almost all of the fuel element behaviors. It is known that the key factors which may affect the temperature distribution of metallic fuel are porosity formation, bond sodium infiltration into

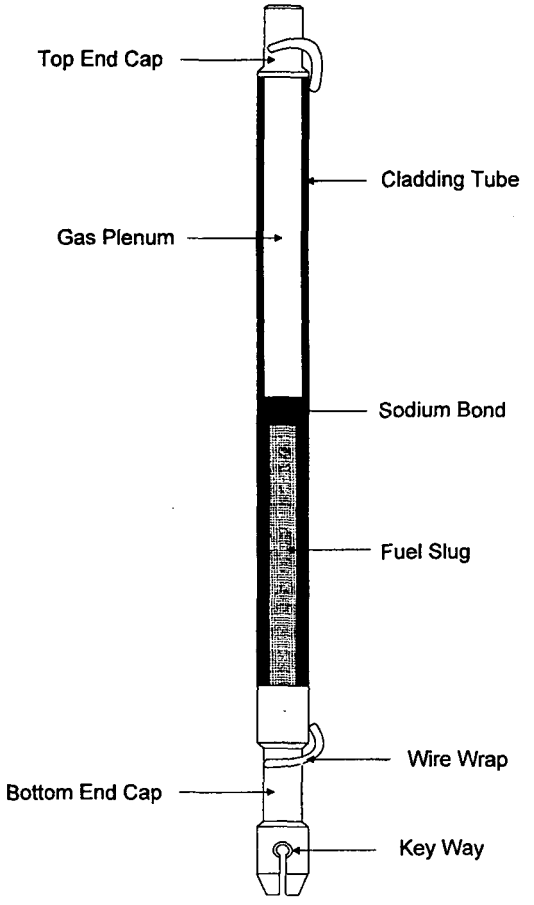

Fig. 1. Sketch of Metallic Fuel Pin for LMRs

the porosity, and fuel constituent migration[3].

As other types of nuclear fuels, the formation of porosities in the metallic fuel also affects its temperature distribution by degrading thermal conductivity of the fuel. Metallic fuel has a tendency that rapid swelling appears at relatively low burnup (1~2 at.%), and then its swelling rate decreases rapidly. The swelling characteristics of metallic fuel are primarily due to the interconnecting phenomena between the porosities. During free-swelling stage (up to 1~2 at.%), large amount of the porosities are developed in the fuel slug. Later, as swelling proceeds, the porosities are interconnected with each other and the fission gases in the porosities are vented to the plenum through the pre-formed porosity network. Eventually, the swelling rate is rapidly decreased after free-swelling stage.

On the other hand, the bond sodium can be infiltrated into the vented porosities. This ingress of high-conductivity bond sodium into the fuel porosity effectively restores much of the thermal conductivity that the fuel lost in the free-swelling stage.

The radial fuel constituent migration related to the formation of three distinct phasal zones is a general phenomenon in the irradiated U-Pu-Zr and U-Zr alloy[4,5]. The thermal conductivity of the U-Zr fuel can be expressed as a function of fuel composition. Therefore, if a constituent migrates, fuel temperature would be changed by thermal conductivity variation as well as heat generation rate variation in the radial direction.

Bauer and Holland[6] studied the effects of porosities and sodium infiltration in irradiated metallic fuel element and obtained a correlation accounting for the effects. Several authors[7,8] have attempted to model and explain the redistribution phenomenon, solving the diffusion equations governed by chemical potential and thermotransport (Soret) effects.

Their basic concepts of redistribution models are similar, but due to the lack of experimental data, it tends to be the less practical of the models. Recently Hofman et al.[9] developed the more realistic redistribution model based on the PIE results of U-10Zr fuel. The Hofman' s model predicted the $\gamma \leftrightarrow (\beta+\gamma)$ and $\gamma \leftrightarrow (\alpha+\gamma)$ phase boundaries occurred at r/R = 0.46, and 0.72, respectively. However, these values were not consistent with the measured data[10] 0.39 and 0.65, respectively.

As the redistribution phenomenon and fuel temperature distribution are affected by each other during irradiation, the combination of the two

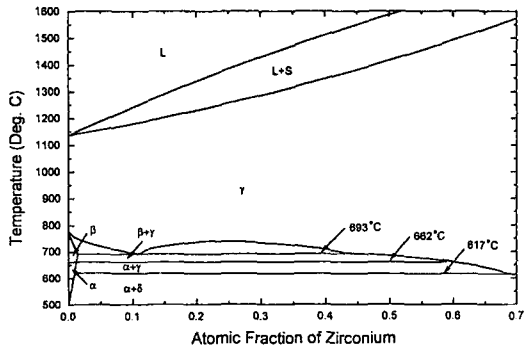

Fig. 2. The Equilibrium Phase Diagram of U-Zr Alloy

models is required. In this work, the constituent redistribution of U-10Zr binary alloy is calculated with using more precise prediction of the pin temperature, and compared with experimental data in open literatures.

Furthermore, the redistribution effect on fuel integrity such as fuel-clad eutectic reaction and solidus temperature variation is discussed.

2. Modeling and Analysis

2.1. Fuel Constituent Redistribution

Fig. 2 shows the equilibrium phase diagram of U-Zr alloy. When an operating temperature of U-Zr fuel is placed over 617℃, it is expected that three phasal zone formation in radial direction of the fuel such as single γ, dual (β+γ) and (α+γ) phase.

In a single-phase binary system, the diffusion flux, J, that is subjected to concentration gradient and temperature gradient is given by[11]

$$J = -\tilde{D}\left(\nabla C + \frac{Q^* C}{RT^2}\nabla T\right) \tag{1}$$

where, $\tilde{D}$ is inter-diffusion coefficient, ∇C is concentration gradient and Q^* is heat of transport which act as driving force for redistribution under temperature gradient, R is universal gas constant and ∇T is temperature gradient. The Eq. (1) is used to calculate the Zr flux in a single-phase region.

Thermotransport behaviors in the two-phase region of several binary alloy systems have been studied to model the dilute interstitial atom migration[12,13], and their theory is employed in this work. The saturation concentration of solute in a phase, Cs, varies with temperature as,

$$C_S = C_0 \exp\left(-\frac{\Delta H_S}{RT}\right) \tag{2}$$

where, ΔHs is partial molar enthalpy of solution. Differentiation of Eq. (2) with radial direction yields,

$$\begin{aligned}\nabla C_S &= C_0 \frac{\partial}{\partial T}\left(-\frac{\Delta H_S}{RT}\right)\nabla T \exp\left(-\frac{\Delta H_S}{RT}\right) \\ &= C_0\left(-\frac{\Delta H_S}{RT}\right)\times\frac{\Delta H_S}{RT^2}\nabla T = C_S\frac{\Delta H_S}{RT^2}\nabla T\end{aligned} \tag{3}$$

Provided local equilibrium condition is achieved spontaneously along to the solubility limit, the concentration gradient of solute in a phase will become the gradient of saturation concentration in Eq. (3). Therefore substitution of Eq. (3) into Eq. (1) gives the expression for the atomic current in a dual-phase field as,

$$J = -\tilde{D}C_S V_f\left(\frac{\Delta H_S + Q^*}{RT^2}\right)\nabla T \tag{4}$$

where volume fraction of γ phase, V_f, is introduced to take account of the volume contribution to diffusion process where the second phase is present. The value of V_f is easily determined from the phase diagram by the lever rule. From the Eq. (3), ΔHs can be expressed as,

$$\Delta H_S = \frac{RT^2}{C_S}\frac{\partial C_S}{\partial T} \tag{5}$$

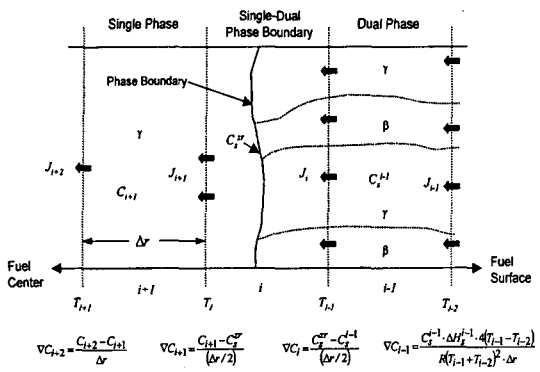

Fig. 3. Calculation Scheme of Zirconium Flux with the Position where the Phase Placed

Thus, the ΔHs also can be determined by evaluating the temperature gradient of saturation concentration from the phase diagram.

To determine the flux between single and two phase region, Marino' s method[14] is applied as follows,

$$J = -\tilde{D}\left(\frac{2(C-C_S)}{\Delta r} + \frac{Q^*C}{RT^2}\nabla T\right) \tag{6}$$

Between Eqs (1), (4) and (6), the calculation of concentration gradient is only difference along to phase condition for the calculation of atomic current. Fig. 3 shows the finite difference form to determine concentration gradient with the radial position where the phase is placed.

It is well known that the dual-phase microstructure of U-Zr alloy has laminar structure. Therefore, for instance, (β+γ) dual-phase region, the phases are stacked sequentially such as $\cdots\beta\gamma\beta\gamma\beta\gamma\beta\gamma\cdots$, for that reason we can assume the Zr flux, Jzr is the sum of flux in β-phase and γ-phase.

$$J_{zr} = J_\gamma + J_\beta$$
$$= -\tilde{D}_\gamma C_s^\gamma V_f\left(\frac{\Delta H_s^\gamma + Q_\gamma^*}{RT^2}\right)\nabla T - \tilde{D}_\beta C_s^\beta(1-V_f)\left(\frac{\Delta H_s^\beta + Q_\beta^*}{RT^2}\right)\nabla T \tag{7}$$

After calculation of the Zr flux using above equations, the Zr concentration change with irradiation time is calculated from continuity equation in cylindrical geometry,

$$C_i^t = C_i^{t-\Delta t} + 2\Delta t\left(\frac{r_i J_i - r_{i+1}J_{i+1}}{r_{i+1}^2 - r_i^2}\right) \tag{8}$$

where Δt is time step and i is the annulus node number.

2.2. Thermal Conductivity Correlations

The thermal conductivity of the unirradiated U-Zr alloy, k_0 (W/mK), is given as a function of temperature and alloy composition[15].

$$k_0 = 17.5\left(\frac{1-2.23Wz}{1+1.61Wz}\right) + 1.54\times10^{-2}\left(\frac{1+0.061Wz}{1+1.61Wz}\right)T + 9.38\times10^{-6}T^2 \tag{9}$$

where, T is the temperature in kelvins and Wz is the weight fraction of zirconium. Generally, the thermal conductivity of U-Zr alloy increases with temperature and decreases with the increment of zirconium content.

To account for the sodium logging as well as porosity effect, Bauer and Holland[6] derived the following porosity correction factor.

$$P_f = \left\{1 - 3\frac{P_{Na}}{(1-P_g)}\frac{\left(1-\frac{k_{Na}}{k_0}\right)}{\left[\frac{2}{\varepsilon} + \left(3-\frac{2}{\varepsilon}\right)\left(\frac{k_{Na}}{k_0}\right)\right]}\right\} \times \left(1-P_g\right)^{3/2} \tag{10}$$

where, k_{Na} is the thermal conductivity of logged sodium, k_0 is the unirradiated fuel thermal conductivity, P_{Na} is the sodium-filled porosity fraction, P_g is the gas filled porosity fraction and ε is 1.72. Therefore the thermal conductivity of irradiated fuel is calibrated as $k = P_f \times k_0$.

The thermal conductivity of sodium, k_{Na}(W/mK), is given as a function of temperature[16].

$$k_{Na} = 93 - 0.0581(T-273.15) + 1.173\times10^{-5}(T-273.15)^2 \tag{11}$$

Table 1. Major Irradiation Conditions and PIE Results of the DP-11 Fuel Pin

Fuel Length	34.3 cm	Burnup (EOL)	7.7 at%
Fuel Slug Radius			
Unirradiated	0.217 cm	Cycle-Averaged Linear Power	242 kW/cm
EOL	0.259 cm		
Effective Full Power Days (EFPD)	619	Cycle-Averaged Fuel Surface Temperature	622 ℃
Porosity Fraction(EOL)			
Outer zone	0.3	Phase Boundary Position (r/R)	
Middle zone	0.35	$\gamma \leftrightarrow (\beta+\gamma)$ transition	0.39
Inner zone	0.31	$\gamma \leftrightarrow (\alpha+\gamma)$ transition	0.65

2.3. Temperature Calculations

The one dimensional steady-state heat conduction equation in cylindrical coordinate is described as,

$$rk\frac{\partial T}{\partial r}+\int_0^r rq'''dr=0 \tag{12}$$

where r is the radial position, T is the temperature, k is the thermal conductivity and q''' is the volumetric heat generation rate.

Eq. (12) could be written directly into finite difference form with assuming linear temperature distribution. However, use of a linear distribution requires a very large number of radial nodes because the actual temperature profile exhibits parabolic distribution. So a parabolic temperature distribution is assumed, and then the temperature gradient can be written as,

$$\frac{\partial T}{\partial r}=2r_i\left(\frac{T_{i+1}-T_i}{r_{i+1}-r_i}\right) \tag{13}$$

Using Eq. (13), the Eq. (12) becomes, in finite difference form as,

$$r_i k_i \frac{2r_i(T_{i+1}-T_i)}{r_{i+1}^2-r_i^2}+\Delta r\sum_{j=1}^{i} r_j q_j'''=0 \tag{14}$$

Solving for T_{i+1},

$$T_{i+1}=T_i+\frac{1}{2k_i}\left[1-\left(\frac{r_{i+1}}{r_i}\right)^2\right]\Delta r\sum_{j=1}^{i} r_j q_j''' \tag{15}$$

Eq. (15) enables the temperature calculation of the fuel pin in which heat generation rate is non-uniformly distributed in the radial direction.

3. Results and Discussion

3.1. Input Data and Calculation Scheme

The DP-11 fuel element(U-10Zr) was irradiated at EBR-II reactor by ANL. The experimental data of the DP-11 pin provide a typical example for verification of this work because these have not only the measured temperature profile[10] but also shows a significant migration of zirconium[9]. The experimental data for fuel temperature were inferred by Yacout et al.[10] from the measurement of radial phase boundaries. They also provided the cycle-averaged fuel surface temperature and linear power, such as 622℃ and 242 kW/cm respectively, using the thermal-hydraulic code Superenergy-2 (SE2). The major irradiation conditions and PIE results of this pin are summarized in Table 1.

A simple correlation on fuel swelling with burnup was made from the curve-fit of PIE results of the pin, and it is used as an input data for simulating the fuel radius change and porosity development. As for linear power and fuel surface temperature, the cycle-averaged values are used as input data. The heats of transport in each phase are inputted as model variables. It is assumed that the heat generation rate at each annulus is linearly proportional to the uranium concentration, which is determined from the fuel constituent redistribution model. The experimental values of diffusion coefficients and heat of transports have not yet been determined in the irradiated U-Zr alloy at temperature range of interesting. Hofman et al.[9] extrapolated the ex-reactor diffusion coefficients down to the (δ+α) temperature range and these correlations are used in our model. The diffusivities of each phase are,

$$D_{\alpha} = 0.002\exp\left(-\frac{170000}{RT}\right) \quad (16)$$

$$D_{\beta} = 0.57\exp\left(-\frac{180000}{RT}\right) \quad (17)$$

$$D_{\gamma} = D_{\gamma 0}\exp\left(-\frac{1000\left(128 - 107X_{zr} + 174X_{zr}^2\right)}{RT}\right) \quad (18)$$

where, $D_{\gamma 0} = 10^{(-2.67 - 8.05X_{zr} + 9.13X_{zr}^2)}$ and X_{zr} is mole fraction of zirconium in gamma phase.

The diffusion coefficient of (α+δ) phase is regarded as same as that of α-phase because the diffusivity of (α+δ) phase has not been measured yet.

The U-Zr phase diagram has been reconstructed by several polynomial equations. From the polynomial equations, phase determination as well as volume fraction and molar enthalpy are evaluated.

The computer program for temperature calculation and redistribution model has been written as separate subroutines. However, the calculation procedure on this work is illustrated in a flow chart (Fig. 4) in order to show its inter-relations between the temperature and redistribution. And this flow chart shows the only one time step of irradiation history. If there are several histories, the procedure will be repeated. After determination of fuel temperature profile, the program determines the phase field at each node from the temperature profile and composition concentrations. After then, the program evaluates the material properties such as molar enthalpy, volume fraction and diffusion

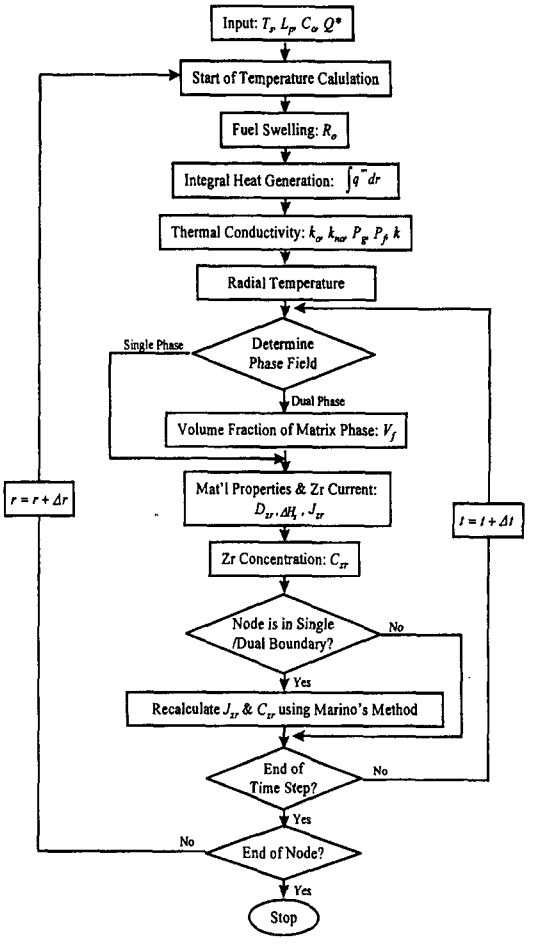

Fig. 4. Flow Chart of the Temperature Prediction Scheme

coefficients, and computes the Zr concentration at each node. For the concentration change with time, explicit time increase is used, and the time step is controlled by diffusion coefficient and node size. The temperature change due to redistribution is small, so the same temperature profile is used within a given time step of irradiation history.

3.2. Fuel Constituent Redistribution

As described before, the driving forces acting on the Zr migration can be divided into 3 terms, i.e., molar enthalpy of solution (ΔH_s) term due to Zr solubility change with radial temperature profile, heat of transport (Q^*) term due to temperature gradient, and concentration gradient term which tends to equalize the concentration distribution. As can be seen in the phase diagram, the molar enthalpy of solution of γ phase in dual phase region has always negative value, thus, the zirconium atom migrates up to the high temperature region.

The diffusion coefficient controls the amount of Zr redistribution, while the ΔH_s and Q^* control the direction and trend of redistribution. Unfortunately, in U-Zr alloy, neither the in-reactor diffusion coefficient nor the heat of transport is known yet. To resolve this problem, firstly the ex-reactor diffusivity is increased until the amount of Zr depletion is coincides with experimental data. In general, mobility of alloying element in irradiated material is higher than that of the unirradiated, due to the existence of large amount of vacancy in irradiated material. Previous researchers could not obtain the desired results unless they assumed the increase of the in-reactor diffusivity by the factor of 10[9] or 70[7] from the ex-reactor value.

In the present study, all the diffusion coefficients are increased to 15 times of ex-reactor

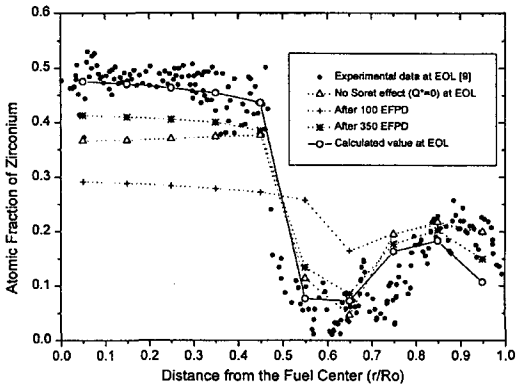

Fig. 5. Comparison of Model Calculation and Experimental Data on Zirconium Redistribution for the Pin DP-11. The Heat of Transport is -50 kJ/mole and 15 Fold Increment of Ex-reactor Diffusivity is Assumed

diffusivities. As shown in Fig. 5, significant amount of zirconium is depleted in the intermediate zone even when Soret effect is ignored. This implies that the solubility effect dominates the redistribution process.

But in the case of $Q^*=0$, the calculated trend of Zr fraction in γ-phase shows a decrease with increasing fuel temperature. This indicates that a negative value of the heat of transport additionally contributes to the redistribution in γ-phase. Thus, under the assumption that $Q^*=-50$ kJ/mole, Q^*_β, $Q^*_\alpha=0$ the predicted redistribution gives good agreement with experimental data. In fact, neither the heats of transport for uranium-rich phase, Q^*_β and Q^*_α, nor the enthalpies of solution for uranium-rich phase ΔH^β_s and ΔH^α_s can affect significantly to the redistribution since the solubility and diffusivity of zirconium on these phases are negligible than those of γ-phase. For a comparison, Sohn et al[17] experimentally determined the heat of transport of ternary U-19Pu-10Zr alloys, and the value for Q^*_γ was $-$

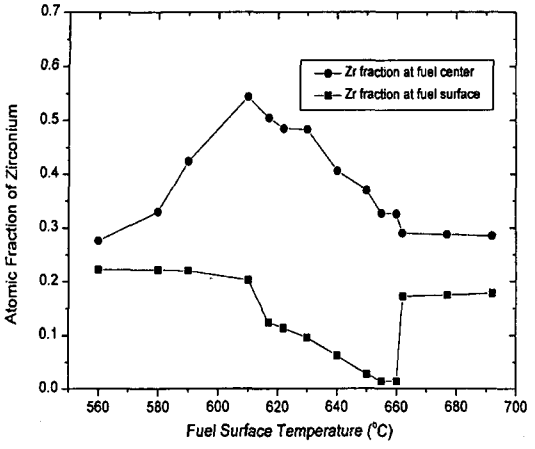

Fig. 6. The Simulated Zr Redistribution of the DP-11 Pin as a Function of Fuel Operating Temperatures

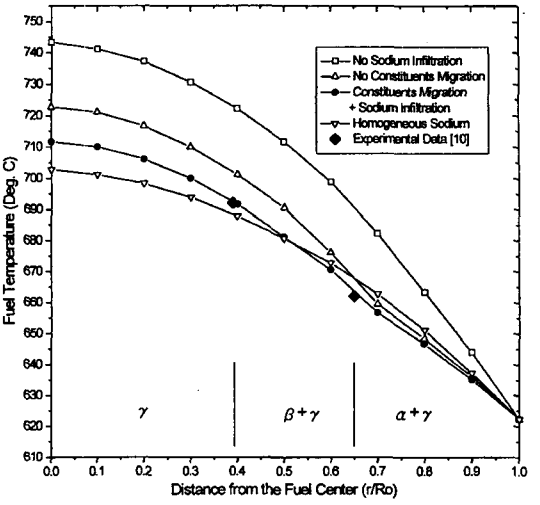

Fig. 7. Comparison of Model Calculation and Experimental Data on Fuel Temperature Distribution at EOL of the Pin DP-11

77 kJ/mole, which is somewhat close to our estimated value −50 kJ/mole. The greater depletion of zirconium and enrichment of uranium in intermediate ($\beta+\gamma$) phase region can be explained by the lower zirconium mobility of ($\alpha+\gamma$) phase than ($\beta+\gamma$) phase. Especially the Zr mobility in β-phase is lower than that in β-phase by two orders of magnitude.

The reason for Zr addition to metallic fuel is to increase melting point of the fuel and to enhance the chemical compatibility between fuel and cladding. In this regard, the fuel constituent redistribution may affect the integrity of fuel pin. Fig. 6 shows the simulated Zr redistribution of the DP-11 pin as a function of fuel operating temperatures. At around 610 ℃ of fuel surface temperature, the model predicts the Zr fraction in fuel center reaches its peak of 0.54, and there will be no centerline Zr depletion expected in all range of temperature. This indicates fuel centerline melting will be retarded as redistribution occurs during off-normal conditions. But Zr depletion at fuel surface may affects deleterious effect on fuel pin integrity. According to the fuel-clad compatibility experiments[18], the eutectic temperature of metallic fuel with 304 SS was around 810℃ when Zr content was above 10 w/o, whereas the temperature was decreased to around 720℃ when 6.3 w/o of Zr alloyed fuel was used. The model predicts that the sharp Zr depletion occurs at fuel surface when the fuel surface temperature is approached the upper limit of ($\alpha+\gamma$) phase boundary. This phenomenon has not been confirmed yet experimentally, but the fuel designers might be carefully attend on this effect for setting up their operating temperature limit.

3.3. Temperature Prediction

As shown in Fig. 7, MACSIS code overestimates the fuel temperature if sodium logging effect is not considered. Pahl et al.[19]

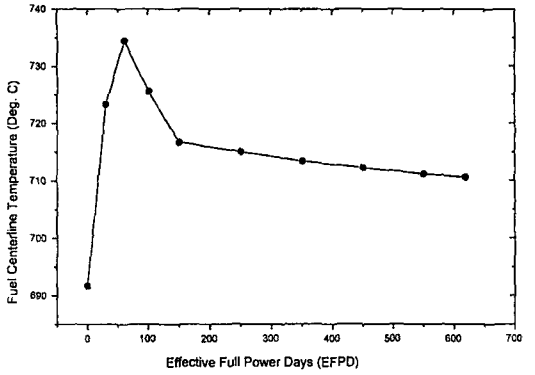

Fig. 8. Prediction for Fuel Center Temperatures of DP-11 Pin as a Function of Irradiation Time

estimated that about 34% of fission gas bubble volume was filled with sodium after irradiation of U-10Zr fuel, by measuring the sodium level decrease in the fuel pin. However, the distribution function of the logged sodium is not known. In the case of the logged sodium is homogeneously distributed in the fuel slug, the temperature gradient in $(\beta+\gamma)$ region is underestimated. It is not reasonable to assume the logged sodium is homogeneously distributed within the fuel slug because it is unlikely that all of the porosities are interconnected with each other up to the innermost zone of the fuel. Furthermore, Liu and Solomon[20] studied experimentally the sodium logging effect of U-Zr alloy based on 'Differential Capillarity' and reported that less sodium penetration was observed at high retained gas pressure. Therefore buildup of fission gas pressure in pores with irradiation will inhibit the sodium wetting into the inner zone of the fuel. The temperature profiles between model calculation and measured data[10] show good agreement under assumption that only the outermost $(\alpha+\gamma)$ region is logged by bond sodium. From this analysis, it seems that the logged bond sodium is concentrated on the outer region of fuel slug.

The temperature profile, with the assumption of no constituent redistribution, exhibits a slight overestimation at $(\beta+\gamma)$ region. As a constituent migrates, the $(\beta+\gamma)$ region becomes uranium enriched zone such that the heat generation rate as well as the thermal conductivity are higher at this zone. However, the conductivity increases more rapidly than heat generation rate with fuel composition change, which results in overall temperature decrease when the redistribution is considered.

Fig. 8 shows the predicted centerline temperatures of the fuel with irradiation time. The rapid increase of the temperature in the early irradiation stage is resulted from the high porosity formation rate during free swelling stage, after then, sodium logging effect restores the thermal conductivity and results in the temperature decrement. The calculation results of fuel temperature variation with irradiation time show good agreement with general trend of metallic fuel temperature variation[3].

4. Conclusions

A temperature calculation scheme of U-10Zr metallic fuel slug has been developed, which covers the effects of constituent redistribution and sodium logging effects.

The calculated Zr redistribution is matched well with experimental data under assumption that 15 times increment of ex-reactor diffusivity and Q^*_γ is -50 kJ/mole. It is apparent that the main driving force for constituent redistribution is the radial solubility gradient of zirconium in γ-phase. The large depletion of zirconium in intermediate $(\beta+\gamma)$ phase region is mainly due to the low zirconium mobility of $(\alpha+\gamma)$ phase region. When the irradiation temperature of fuel surface is maintained within $(\alpha+\gamma)$ and $(\beta+\gamma)$ phase range,

the centerline melting temperature of U-10Zr fuel will be increased, but eutectic temperature at fuel surface will be decreased.

From the comparison of temperature calculation and measured, it seems that the bond sodium would not be homogeneously distributed but concentrated in the outer region of the fuel slug. The redistribution effect on the temperature profile is not so great because increase of heat generation rate compensates for the thermal conductivity increase where the zirconium depleted zone.

References

1. B. R. Seidel, et al., "A Decade of Advances in Metallic Fuels", *ANS Meeting*, Washington D. C. (1990).
2. W. Hwang, C. Nam, J. S. Yim, Y. C. Kim and M. Cho, "Development Status of MACSIS Code for Simulating the In-Reactor Behavior of Metallic Fuel", *Proceedings of ICONE 5*, Nice, France (1997).
3. G. L. Hofman, L. C. Walters and T. H. Bauer, "Metallic Fast Reactor Fuels", *Progress in Nuclear Energy*, **31**, 83 (1997).
4. F. Murphy, W. N. Beck, F. L. Brown, B. J. Koprowski and L. A. Neimark, "Postirradiation Examination of U-Pu-Zr Fuel Elements Irradiated in EBR-II to 4.5 Atomic Percent Burnup", *ANL-7602* (1969).
5. D. L. Porter, C. E. Lahm, and R. G. Pahl, "Fuel Constituent Redistribution During the Early Stages of U-Pu-Zr Irradiation" , *Metallurgical Transactions*, **21A**, 1871 (1990).
6. T. H. Bauer and J. W. Holland "In-Pile Measurements of the Thermal Conductivity of Irradiated Metallic Fuel", *Nuclear Technology*, **110**, 407 (1993).
7. T. Ogawa, T. Iwai and M. Kurata, "Demixing of U-Zr Alloys Under a Thermal Gradient", *J. of the Less-Common Metals*, **175**, 59 (1991).
8. M. Ishida, T. Ogata and M. Kinoshita, "Constituent Migration Model for U-Pu-Zr Metallic Fast Reactor Fuel" , *Nuclear Technology*, **104**, 37 (1993).
9. G. L. Hofman, S. L. Hayes, M. C. Petri, "Temperature Gradient Driven Constituent Redistribution in U-Zr Alloys", *J. of Nuclear Materials*, **227**, 277 (1996).
10. A. M. Yacout, W. S. Yang, G. L. Hofman and Y. Orechwa, "Average Irradiation Temperature for the Analysis of In-Pile Integral Measurements", *Nuclear Technology*, **115**, 61(1996).
11. P. G. Shewmon, "Diffusion in Solids", McGraw-Hill Book Co., (1963).
12. D. Jaffe and P. G. Shewmon, "Thermal Diffusion of Substitutional Impurities in Copper, Gold and Silver", *Acta Metallurgica*, **12**, 515 (1964).
13. S. C. Axtell and O. N. Carlson,"A Study of the Thermotransport Behavior of Cobalt in Thorium", *Metallurgical Transactions*, **21A**, 2141 (1990).
14. G. P. Marino, "A Numerical Calculation of the Redistribution of an .Interstitial Solute in a Thermal Gradient", *Nuclear Science and Engineering*, **49**, 93 (1972).
15. M. C. Billone, Y. Y. Liu, E. E. Gruber, T. H. Hughes and J. M. Kramer, "Status of Fuel Element Modeling Codes for Metallic Fuels", *Proc. ANS Conf. Reliable Fuels for LMRs*, Tucson (1986).
16. G. H. Golden and J. D. Tokar, "Thermophysical Properties of Sodium", *ANL-7323* (1967).
17. Y. H. Sohn, M. A. Dayananda, G. L. Hofman, R. V. Strain and S. L. Hayes, "Analysis of Constituent Redistribution in γ

U-Pu-Zr Alloys under a Temperature Gradient", to be published in *J. of Nuclear Materials*.

18. C. M. Walter, L. R. Kelman and S. T. Zegler, "Compatibility of U-Pu-Zr and U-Pu-Ti Alloys with Potential Cladding Materials", *ANL-7155*, Part I (1965).
19. P. G. Pahl, C. E. Lahm, R. Villareal, W. N. Beck and G. L. Hofman., "Recent Irradiation Tests of Uranium-Plutonium-Zirconium Metal Fuel Elements", *Proc. ANS Int. Conf. on Reliable Fuels for LMRs*, Tucson, 3-36 (1986).
20. W. Liu and A. A. Solomon, "Liquid Sodium Intrusion into Porous U-10Zr Fuel Alloy by Differential Capillarity", Purdue University (1992).